Eur. Phys. J. D **24**, 361–364 (2003)
DOI: 10.1140/epjd/e2003-00178-5

THE EUROPEAN PHYSICAL JOURNAL D

Silver diffusion and precipitation of nanoparticles in glass by ion implantation

M. Dubiel[1,a], H. Hofmeister[2], G.L. Tan[2], K.-D. Schicke[2], and E. Wendler[3]

[1] Martin-Luther University of Halle-Wittenberg, Department of Physics, Friedemann-Bach Platz 6, 06108 Halle, Germany
[2] Max Planck Institute of Microstructure Physics, Weinberg 2, 06120 Halle, Germany
[3] Institute of Solid State Physics, University of Jena, 07743 Jena, Germany

Received 10 September 2002
Published online 3 July 2003 –

Abstract. Silver particles in soda-lime glass, less than 10 nm in size, were prepared by ion implantation. The implantation dose was in the range of 0.5 to 2×10^{16} Ag ions/cm^2 and the beam current density was varied from 0.5 to 2 μA/cm^2. Here, the beam current density strongly influences ion diffusion and particle precipitation as well as compressive stress generation around the particles due to thermal effects resulting from the deceleration of silver ions. Stress relaxation can be achieved by increased dose rates or thermal processing at elevated temperatures. Based on RBS and HREM results, a possible route to homogeneous distribution of Ag nanoparticles within the glass is discussed with respect to their interesting optical properties.

PACS. 61.80.-x Physical radiation effects, radiation damage – 61.46.+w Nanoscale materials: clusters, nanoparticles, nanotubes, and nanocrystals

1 Introduction

Nanosized metal particles embedded in glass have attracted much interest as material with potential application for optical devices. A number of methods are currently used to incorporate such particles into glassy hosts. Ion implantation enables to introduce high concentrations of different ions into a near-surface region. This way, specific linear and non-linear optical properties, *e.g.*, large third-order non-linear optical susceptibility, can be achieved [1–5]. The resulting macroscopic properties strongly depend on the materials used as well as the preparation procedure. For nanoparticles of Au, Ag or Cu the preparation influences particle size, size distribution and lattice structure.

Usually, an increasing concentration of particles with increasing implantation dose was found, however, the spatial distribution of particles is often changed [6,7]. Elevetad substrate temperature during ion implantation or subsequent thermal processing speed up diffusion and precipitation processes resulting, *e.g.*, in a bimodal depth distributions of nanoparticles with their highest concentration at the maximum of radiation damage and at the maximum penetration depth [6,8–10]. A dissolution of larger particles and this way a narrowing of size distribution could be achieved by applying laser pulse irradiation, although this will not produce a Gaussian shape of distribution [6,11]. By varying the beam current density between 200 nA/cm^2 and 1–2 μA/cm^2 a modification of the depth distribution was found for silver in lithia-alumina-silica glass [8]. Likewise, the third-order susceptibility of copper particles in SiO_2 has been changed by dose rate variations of 1–100 μA/cm^2 [5]. This points to a specific role of the beam current density in ion implantation.

The aim of the present work was to study the effects of both implanted dose and ion beam current density on diffusion processes and the formation of silver nanoparticles. The structural characterization by means of high resolution electron microscopy should reflect the interaction of crystalline precipitates with the surrounding amorphous matrix. Rutherford backscattering was used as analytical tool for determining the spatial distribution of silver atoms and ions within the glass.

2 Experimental

Commercial soda-lime glass containing (in mole%) 72.4% SiO_2, 14.4% Na_2O, 6.4% CaO, 6.0% MgO, 0.5% Al_2O_3, 0.20% K_2O, 0.3% SO_3 and 0.04% Fe_2O_3 was used as substrate. Implantation of Ag^+ ions of 200 keV energy was performed at room temperature to doses of 0.5×10^{16}, 1.0×10^{16} and 2×10^{16} ions/cm^2. On the glass of 1 mm thickness an area of 20×10 mm^2 was subjected to implantation. Further on, the beam current density was varied in the range of 0.5 to 2 mA/cm^2. To reduce charge buildup

[a] e-mail: dubiel@physik.uni.halle.de

during implantation the glass surface was additionally exposed to electron beam irradiation. The spatial distribution of glass constituents, especially the depth distribution of Ag species, was determined by Rutherford backscattering spectroscopy (RBS) using 1.4 and 1.5 MeV He^+ ions, respectively.

Electron microscopy examination to estimate size, size distribution and depth distribution of silver particles was done by means of a JEM 1010 operating at 100 kV. To this aim planar and cross-section preparation was required including mechanical grinding, polishing and ion-beam etching. For advanced structural characterisation a high-resolution electron microscope (HREM) operating at 400 kV (JEM 4010) was used. Lattice parameters of individual Ag particles were determined from digitised HREM micrographs by image processing (real space and diffractogram evaluation) using the Digital Micrograph (GATAN) and NIH Image software [12]. For this evaluation only images of single crystalline particles have been considered which mostly displaid {111} and/or {200} lattice planes according to a face centered cubic structure.

3 Spatial distribution of silver species by RBS

Previous experiments [13] have shown that Ag^+ ion implantation (200 keV) at a beam current density as low as about 1 $\mu A/cm^2$ causes Ag precipitation even at room temperature regardless of the implantation dose. The bimodal depth distribution observed in all cases is due to diffusion of highly mobile silver species away from the maximum position of the ion stopping range towards the surface and the interior of the glass. In lithia-alumina-silica glass Arnold and Borders observed the usual Ag depth distribution of Gaussian shape, however, only at low temperatures (77 K) and reduced beam current density (200–300 nA/cm^2) [8]. Accordingly, for the soda-lime glass studied here we reduced the beam current density to 0.5 $\mu A/cm^2$ what resulted in a nearly Gaussian depth distribution as may be deduced from the open circles spectrum in Figure 1. An increase of the dose to 2×10^{16} Ag^+ ions/cm^2 already leads to a non-symmetric depth distribution of silver species as indicated by the filled circles spectrum in Figure 1.

Enhancement of the beam current density to 2 $\mu A/cm^2$, on the other hand, results in a bimodal depth distribution of Ag species as can be seen from Figure 2, similar to that found previously for 1 $\mu A/cm^2$ [13]. These findings confirm the assumption of Arnold and Borders [8] that the beam current applied during ion implantation sensitively influences the ion-beam heating effect. The temperature in the implanted region increases, especially in the case of high local Ag concentration, because of the impact of collisional energy in the course of ion deceleration.

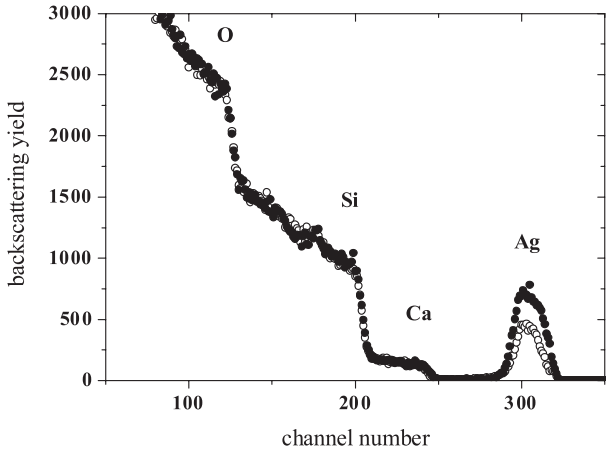

Fig. 1. RBS (1.4 MeV He^+ ions) spectra of Ag^+ ion implanted glass (beam current density: 0.5 $\mu A/cm^2$, dose: open circles 1×10^{16}, and filled circles 2×10^{16} ions/cm^2).

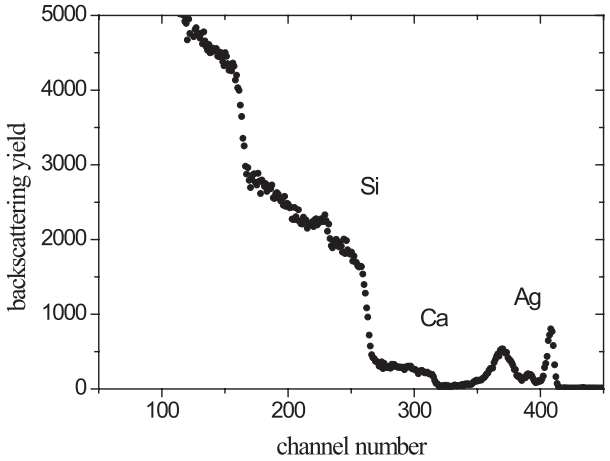

Fig. 2. RBS (1.5 MeV He^+ ions) spectrum of Ag^+ ion implanted glass (beam current density: 2 $\mu A/cm^2$, dose: 1×10^{16} ions/cm^2).

4 Structural characterisation by electron microscopy

The spatial distribution of precipitated silver nanoparticles and their structural characteristics was studied by electron microscopy. From TEM investigation and also from optical spectroscopy it is obvious that upon implantation at low beam current density (0.5 $\mu A/cm^2$) less Ag particles are precipitated, *i.e.* most of the implanted silver remains in ionic or atomic state because of the lower supersaturation. The arrangement of silver nanoparticles beneath the surface across the glass can be imaged using cross-section preparation. The depth profile of particles in the glass exposed to implantation with increased beam current density (2 $\mu A/cm^2$) is similar to the bimodal depth distribution of silver species revealed by the RBS spectrum. The glass implanted to 2×10^{16} Ag ions/cm^2 exhibits two layers parallel to the surface that contain silver particles. The near-surface one at a depth of about 40 nm shows larger particles, while a second layer is formed

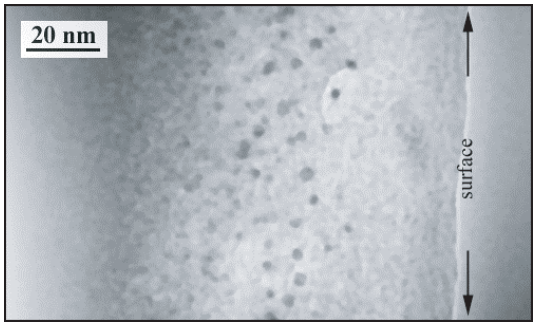

Fig. 3. Cross-section image of the glass implanted to a dose of 1×10^{16} ions/cm^2 (200 keV).

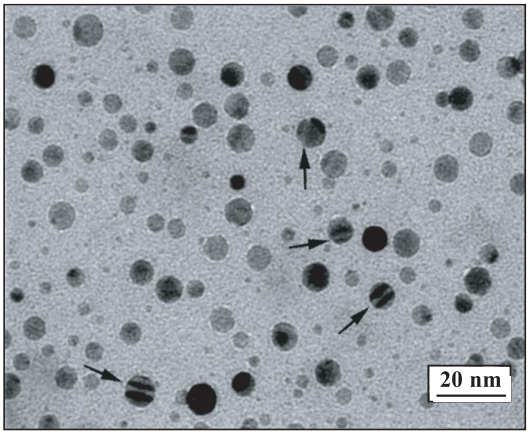

Fig. 4. Plane-view image of the glass implanted to a dose of 2×10^{16} ions/cm^2 (200 keV).

around 100 nm below the surface. The mean size of silver nanoparticles amounts to about 6.9 nm. For the lower implantation dose of 1×10^{16} Ag ions/cm^2 these particle layers, especially the near-surface one, are not well established, similar to the results previously observed for implantation at 1 μA/cm^2 beam current density [13]. The mean particle size of the 1×10^{16} Ag ions/cm^2 sample amounts to about 3.2 nm. This difference is due to the lower total amount of implanted silver as well as to the reduced thermal effects. The above mentioned results may be illustrated by Figure 3 showing the cross-section of the 1×10^{16} Ag ions/cm^2 sample and Figure 4 showing the planar image of the 2×10^{16} Ag ions/cm^2 sample where arrows point to lattice defects in the particles. These lattice defects apparently are not related to the beam current density, but to the implantation dose.

In addition to their general structural characteristics, lattice analysis by means of HREM images may reveal the stress state of Ag nanoparticles in glass and this way also the stress state of the surrounding matrix. Since for the sample implanted at rather low beam current density (0.5 μA/cm^2) without any additional processing only much less particles are detectable, no reliable lattice parameter data are available up to now. Ion implantation at a beam current density of 1 μA/cm^2 resulted in a strong compressive stress acting on the particles as indicated by severe lattice contractions regardless of the

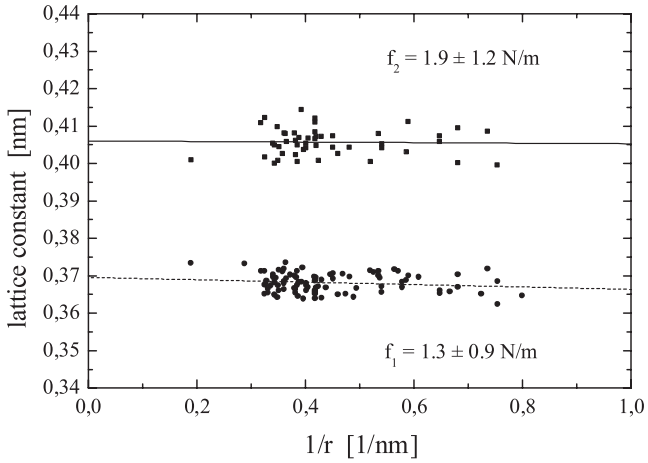

Fig. 5. Lattice parameter of silver particles in glass, lower curve: as implantated, upper curve: upon annealing at 400 °C (implantation dose: 2×10^{16} Ag$^+$ ions/cm^2, beam current density: 1 μA/cm^2).

particle size [13]. This effect was explained by the local increase of mass density within the implanted region at the maximum of ion stopping range around 100 nm depth for Ag$^+$ ions of 200 keV energy. The observed stress could be relaxed by thermal processing at elevated temperatures. That is shown in Figure 5 comparing lattice parameter *versus* reciprocal particle size plots of the as implanted and the 400 °C annealed sample. The lattice parameters all together jump to the bulk value while nearly no change of the size dependence, expressed by the interface stress f (corresponding to the surface stress of free particles) [14,15], is observed. It should be noted here that TEM as well as RBS spectra of the annealed samples reveal a strong dissolution of silver particles and a broadening of the spatial distribution of silver species. Thus, a stress induced dissolution of particles and a corresponding diffusion out of the stress region is to be considered.

This extensive lattice contraction was not observed for implantation at room temperature with higher beam current density (2 μA/cm^2). To demonstrate this Figure 6 shows the corresponding plot of lattice parameters *versus* reciprocal particle size. It is assumed that thermal effects owing to the increased beam current density allow for immediate stress relaxation.

5 Conclusions

Diffusion and precipitation processes in Ag$^+$ ion implanted soda-lime glass have been investigated by means of RBS and electron microscopy. It was found that a symmetric depth distribution of Ag species of Gaussian shape can be realized only for low beam current densities of 0.5 μA/cm^2 using an implantation dose not higher than 1×10^{16} Ag ions/cm^2. It can be assumed that both process parameters influence the diffusion behaviour. The thermal effects are determined by the beam current density while the implantation dose determines the exposure time

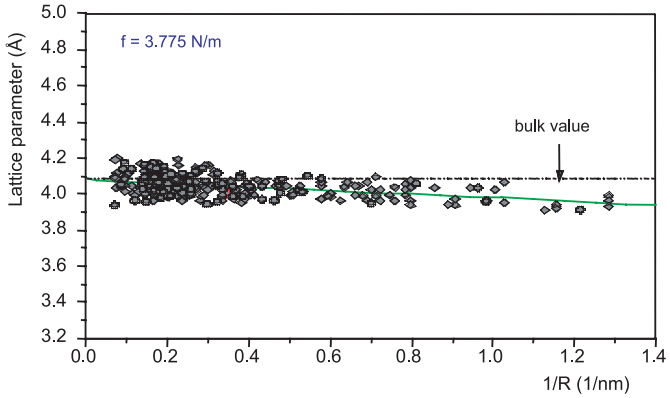

Fig. 6. Lattice parameter of silver particles in glass, as implantated (implantation dose: 2×10^{16} Ag^+ ions/cm^2, beam current density: 2 μA/cm^2).

and this way the available time for movement of ions and atoms.

The unusual stress behaviour is unambiguously determined by the beam current density applied during implantation. HREM lattice analysis demonstrated that dose rates of 2 μA/cm^2 yield a relaxed state of nanoparticles and surrounding glass matrix. The compressive stress generated by low-dose rate implantation causes dissolution of particles and additional diffusion upon annealing at 400 °C. Usually, a temperature increase leads to further particle formation [6,8–10] and only near the glass transformation temperature dissolution occurs.

A homogeneous distribution of Ag nanoparticles with respect to size and depth can be achieved most probably only at low temperatures [8]. In any case, a temperature increase causes diffusion and precipitation processes resulting in the formation of a second near-surface layer of particles the sizes of which are different to those already precipitated. Application of pulsed laser irradiation could be a way of narrowing the size distribution [6,11].

The stress states as well as diffusion and precipitation effects discussed are expected to strongly influence the optical properties of Ag nanoparticles in the glass as it was observed for similar systems [5,7]. That is why efforts are in progress now to study also optical properties of the materials.

This work has been supported by Deutsche Forschungsgemeinschaft (SFB 418).

References

1. K. Fukumi, A. Chayahara, K. Kadono, T. Sakaguchi, Y. Horino, M. Miya, K. Fuji, J. Hayakawa, M. Satou, J. Appl. Phys. **75**, 3075 (1994)
2. R.H. Magruder III, R.A. Zuhr, D.H. Osborne Jr, Nucl. Instr. Meth. B **99**, 590 (1995)
3. F. Gonella, Nucl. Instr. Meth. B **166-167**, 831 (2000)
4. S.S. Sarkisov, E. Williams, M. Curley, D. Ila, P. Venkateswarlu, D.B. Poker, D.K. Kensley, Nucl. Instr. Meth. B **141**, 294 (1998)
5. Y. Takeda, J.P. Zhao, C.G. Lee, V.T. Gritsyna, N. Kishimoto, Nucl. Instr. Meth. B **166-167**, 877 (2000)
6. A.L. Stepanov, D.E. Hole, Recent Res. Devel. Appl. Phys. **5**, 1 (2002)
7. Z. Liu, H. Li, X. Feng, S. Ren, H. Wang, Z. Liu, B. Lu, J. Appl. Phys. **84**, 1913 (1998)
8. G.W. Arnold, J.A. Borders, J. Appl. Phys. **48**, 1488 (1977)
9. R.A. Wood, P.D. Townsend, N.D. Skelland, D.E. Hole, J. Barton, C.N. Alonso, J. Appl. Phys. **74**, 5754 (1993)
10. D.E. Hole, A.L. Stepanov, P.D. Townsend, Nucl. Instr. Meth. B **148**, 1054 (1999)
11. A.L. Stepanov, D.E. Hole, P.D. Townsend, Nucl. Instr. Meth. B **166-167**, 882 (2000)
12. W. Rasband, "NIH Image" public domain software, US National Institute of Health (FTP: `zippy.nimh.nih.gov`)
13. M. Dubiel, H. Hofmeister, E. Schurig, E. Wendler, W. Wesch, Nucl. Instr. Meth. B **166-167**, 871 (2000)
14. C.W. Mays, J.S. Vermaak, D. Kuhlmann-Wilsdorf, Surf. Sci. **12**, 134 (1968)
15. M. Dubiel, H. Hofmeister, E. Schurig, Recent Res. Devel. Appl. Phys. **1**, 69 (1998)